International Journal of Modern Physics A
Vol. 36, Nos. 11 & 12 (2021) 2140003 (16 pages)

DOI: 10.1142/S0217751X21400030

Preliminary simulation analysis of the temperature fluctuation effect on Taiji-1 laser interferometer

Xiaoqin Deng[*,†], Ran Yang[†,‡,§] and Yu Niu[†,‡,¶]

[*] *Changchun Institute of Optics, Fine Mechanics and Physics, Chinese Academy of Sciences(CAS), Changchun 130033, China*

[†] *Taiji Laboratory for Gravitational Wave Universe (Beijing/Hangzhou), University of Chinese Academy of Sciences (UCAS), Beijing 100049, China*

[‡] *Center for Gravitational Wave Experiment, National Microgravity Laboratory, Institute of Mechanics, Chinese Academy of Sciences (CAS), Beijing 100190, China*

[§] *yangran@imech.ac.cn*
[¶] *niuyu@imech.ac.cn*

[‖] *On behalf of The Taiji Scientific Collaboration*

Received 15 September 2020
Revised 16 October 2020
Accepted 30 October 2020
Published 22 March 2021

Space-borne gravitational wave detection imposes a demanding requirement on the sensitivity of the laser interferometer. Among all disturbances that affect the measurement accuracy of the laser interferometer, temperature fluctuations contribute significantly. In this paper, the structure model and the interference path design of Taiji-1 laser interferometer have been used to conduct a preliminary simulation analysis of the temperature fluctuation noise through the finite element method. The temperature, the displacement and the optical path difference fluctuations have been obtained and theoretically analyzed. The preliminary simulation results are consistent with the theoretical analysis, which shows that the thermal–structural–optical simulation scheme adopted in this paper is reasonable. With the preliminary simulation results and the actual temperature control of Taiji-1 laser interferometer, we estimate that in Taiji-1 laser interferometer system, the temperature fluctuation is below the order of mK, the node displacement is within 100 pm, and the interference arm length difference fluctuation amplitude of the laser interferometer is also within 100 pm.

Keywords: Gravitational wave detection; laser interferometer; temperature fluctuation noise; numerical simulaton.

[§,¶]Corresponding authors.
[‖]For more details, please refer to article 2102002 of this Special Issue.

1. Introduction

The basic conception of a space-borne gravitational wave observatory is to arrange three spacecrafts into an equilateral triangle, which forms three nonindependent Michelson interferometers.[1] With a high-precision laser interferometer to measure the distance among the free-falling test masses (TMs), the gravitational wave signal could be converted into the change of the distance between the TMs, as proposed in LISA[2–4] and Taiji program.[5–7] However, the tiny distance fluctuation between the TMs caused by the gravitational wave is hard to be detected,[2] which puts forward a demanding requirement on the sensitivity of the laser interferometer. For example, in the sensitive frequency band of Taiji program at 1 mHz, for two TMs separated by 3×10^6 km, the distance fluctuation between them caused by the gravitational wave with an intensity of 10^{-21} is 10 pm, and the sensitivity requirement of the laser interferometer is $8\,\mathrm{pm/Hz^{1/2}}$.[5,6,8]

The sensitivity of the laser interferometer is affected by a variety of disturbances, of which the coupling of the low-frequency temperature fluctuations to component performance cannot be ignored.[9–14] The general method of suppressing temperature fluctuation noise is to control the system temperature fluctuation through thermal design.[15,16] With the structural design and material selection, the temperature fluctuation noise meets the pre-allocated noise requirement.[12,17,18] However, the effect of the temperature fluctuation noise cannot be completely eliminated via this method. Therefore, it is also necessary to analyze the influence of the temperature fluctuation on the output signal of the laser interferometer, and find the transfer function between the system temperature and the output signal,[19,20] to further minimize even eliminate the temperature fluctuation noise.

Taiji-1 is a Chinese mission to prove the feasibility of the future space-borne gravitational wave observatories, aiming to complete the first on-orbit test of the payloads and the key satellite technologies needed for Taiji program.[5] One of the key payloads on board Taiji-1 is the laser interferometer, and the on-orbit test results have shown that the displacement measurement accuracy of the laser interferometer reaches $100\,\mathrm{pm/Hz^{1/2}}$. In this paper, we use the structure model and optical path design of Taiji-1 laser interferometer to conduct a preliminary simulation analysis of the effect of the temperature fluctuation on the output signal of the laser interferometer.

2. Temperature Fluctuation Noise of Taiji-1 Laser Interferometer

2.1. *The heat transfer mode in Taiji-1 laser interferometer*

In space, the heat transfer modes in Taiji-1 laser interferometer consist of the heat conduction and the heat radiation.

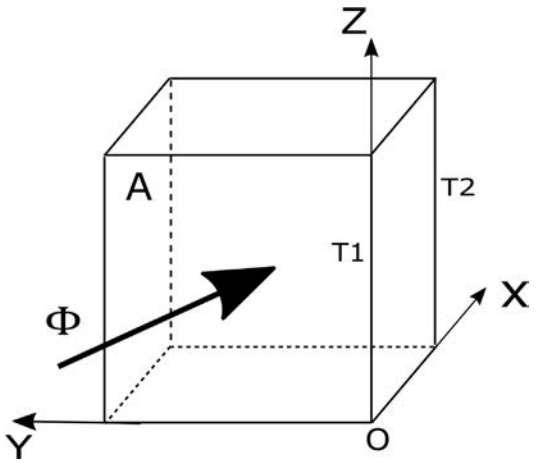

Fig. 1. One-dimensional plate heat transfer.

2.1.1. *Heat conduction*

In the laser interferometer system, the heat inside each component would be transferred from the high temperature part to the low temperature part, and the high temperature component would transfer the heat to the component with low temperature in contact with it.

The heat conduction is ruled by *Fourier's law*.[21] If we consider the one-dimensional heat conduction problem shown in Fig. 1, both surfaces maintain a uniform temperature during the heat conduction, and the temperature only changes in the x direction. For any micro-layer with a thickness of dx in the x direction, according to *Fourier's law*, the conduction heat through the layer per unit time is proportional to its local temperature change rate and the area of the plate, as

$$\phi = -\lambda A \frac{dT}{dx}, \tag{1}$$

where λ (W/m $\cdot$ K) is the thermal conductivity, which is used to characterize the thermal conductivity of the material, A is the area of the plate, and $\phi(W)$ is the heat flow.

2.1.2. *Heat radiation*

In vacuum environment, heat radiation is the most effective mode of heat transfer. All objects are emitting heat radiation to the surrounding space constantly, while absorbing the radiant energy emitted by other objects continuously.

Black body refers to an ideal object that can absorb all radiant energy input to its surface, whose capacity of absorption and radiation is the largest among objects at the same temperature. The radiant energy emitted by a black body per unit time is ruled by *Stefan–Boltzmann's law*[21] as follows:

$$\phi = A\sigma T^4, \tag{2}$$

where $\sigma = 5.67 \times 10^{-8}$ $(\mathrm{W/m^2 \cdot K^4})$ is the Stefan–Boltzmann constant, A is the radiation surface area and T is the thermodynamic temperature of the body. However, the calculation of the radiant heat flow of the actual object can adopt the empirical correction form of the law:

$$\phi = \varepsilon A\sigma T^4, \tag{3}$$

where ε is the emissivity, a parameter related to the surface type and surface state of the object and the value is less than 1.

2.2. *The temperature fluctuation noise generation mechanisms of the laser interferometer system*

In the laser interferometer system of Taiji-1, optical components are mounted on an optical platform of highly stable optical properties. Temperature fluctuations basically affect the laser interferometer system through three mechanisms[13]:

(i) Temperature changes cause dilatation and contraction of the optical platform and the optical components mounted on it, which in return causes the optical path to change accordingly.
(ii) The refraction index of the optical components changes with the temperature fluctuation.
(iii) If the thermal expansion coefficient is different among the optical component and the optical platform and the frame, the refraction index of the optical components will change due to the thermal stress.

Among the three mechanisms, the first mechanism contributes the most to the temperature fluctuation noise. Therefore, in this paper, we have made a preliminary simulation analysis mainly focusing on the effect of the thermal dilatation and contraction of the optical platform and optical component on the output signal of Taiji-1 laser interferometer.

3. The Numerical Simulation

In order to find the characteristics of the temperature fluctuation noise in Taiji-1 laser interferometer system, we adopted a virtual external heat source. The responses of the system temperature, the structure and the optical path of the laser interferometer under the action of an external heat source were simulated through ANSYS and ASAP via the finite element method.

3.1. *The interference path design and the finite element model of Taiji-1 laser interferometer*

There are four interference paths designed in Taiji-1 laser interferometer system. Their specific distribution is shown in Fig. 2: (a) represents two equal-arm reference interference paths with a spatial symmetrical design, which could be used to measure the noise of the optical platform and the fiber jitter caused by the temperature fluctuations; (b) is the TM reference interference path, and the length difference of its interference arms is a constant, mainly used to measure the noise caused by the frequency fluctuations; (c) is the test interference path, used to measure the movement of the TM relative to the spacecraft, and the length difference of its interference arms is also a constant when the TM remains stationary. The overall design of the interference path is shown in the top plot in Fig. 2.

According to the structure and the interference path design of the laser interferometer, a finite element model of Taiji-1 laser interferometer has been established as shown in Fig. 3.

3.2. *Numerical simulation*

In our simulation, a thin plate was placed outside the laser interferometer system as an external heat source. There would be heat radiation between the external heat

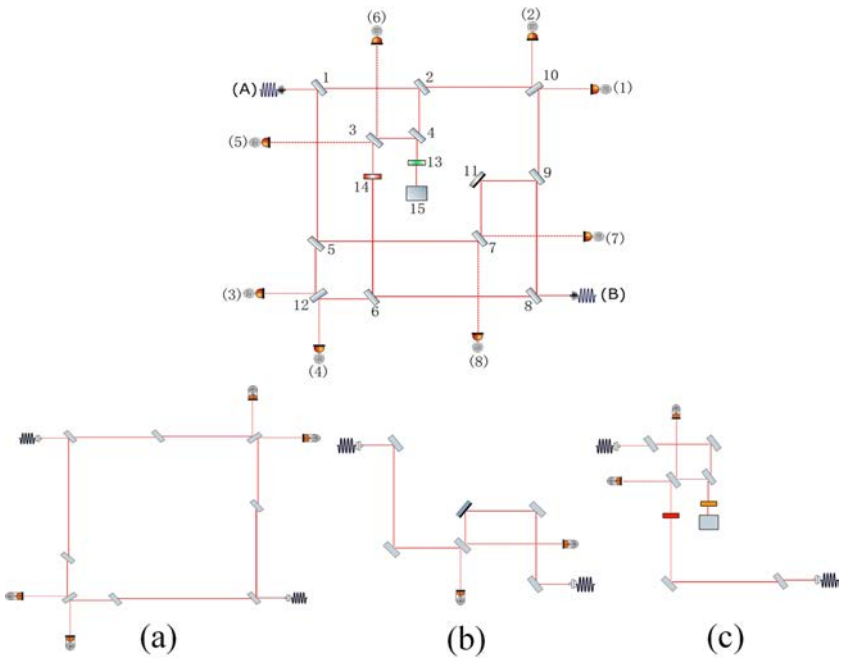

Fig. 2. The interference path design of Taiji-1 laser interferometer. *Top*: The overall design of the interference path. *Lower plot*: (a) two equal-arm reference interference paths; (b) the TM reference interference path and (c) the test interference path.

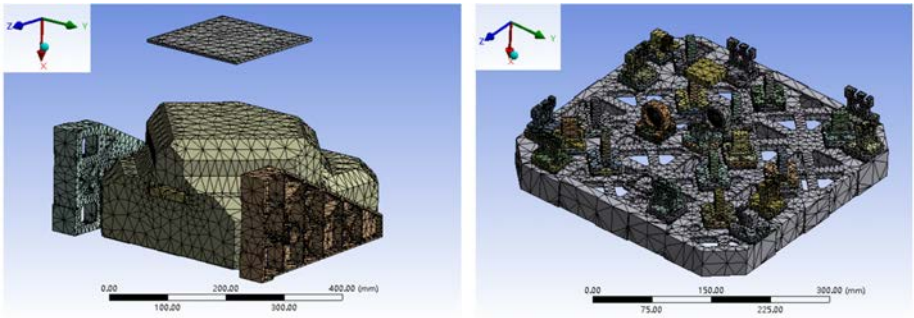

Fig. 3. *Left*: The finite element model of Taiji-1 laser interferometer. *Right*: The finite model of the optical platform, when the thermal shield is hidden.

source and the laser interferometer system, and heat conduction and heat radiation among the internal components. The temperature of the external heat source was set as $T = 293.0 + \Delta T \cdot \cos(2\pi \cdot 0.1 \cdot \text{time})K$, and the initial temperature of the system was 293 K. The heat source temperature amplitude ΔT was variable. Eight units in different key positions were selected as the temperature measurement points, they were located at two laser sources, optical platform, TM housing, TM, the surface of the prism and the brackets on both sides. The four adjacent geometric points in the center of the optical platform were used as the fixed constrains for the transient thermal–structural simulation analysis.

According to the interference path design of Taiji-1 laser interferometer, the original optical model of the laser interferometer was established in ASAP. With the results of transient thermal–structural numerical simulation in ANSYS, the geometric optical path of each interferometer was traced. By subtracting the optical path of the two laser beams arriving at the same detector, the change of the interference arm length difference over time was obtained finally. By changing the temperature amplitude of the external heat source, the relationship between the interference arm length difference and the temperature amplitude was obtained through preliminary simulation analysis.

4. Results and Analysis

According to the above numerical simulation scheme, the system responses of Taiji-1 laser interferometer under the action of the external heat source were obtained through simulation. In this section, we presented the analysis of the numerical simulation results of the temperature, the deformation and the interferometer arm length difference of the laser interferometer.

4.1. *Temperature response of the laser interferometer*

Figure 4 shows the temperature time-domain changes and frequency-domain responses of the eight temperature measurement points, under the same external

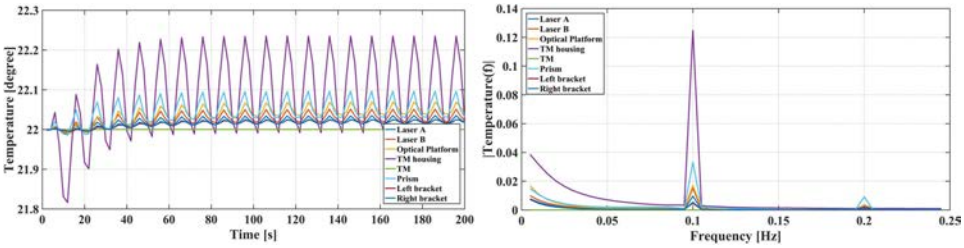

Fig. 4. The temperature amplitude of the external heat source is 20 K. *Left*: The temperature change curves of eight temperature measurement points with time. *Right*: The amplitude spectrum curves after the fast Fourier transform of the temperature data (since the response amplitude is too big at 0 Hz, it is not shown in the plot).

heat source temperature amplitude, and some laws of the system temperature change could be observed through it.

(i) The time-domain temperature curve of each temperature measurement point exhibits a cosine function form corresponding to the heat source.
(ii) The temperature frequency-domain response curves all have a peak at 0.1 Hz, which is the same as the frequency of the heat source.
(iii) The time-domain temperature curves of the temperature measurement points show an obvious drift during the first period of time, and reach stable after some time. In addition, during the initial stage, there is an abrupt change in time-domain and a large response in frequency-domain at zero frequency.
(iv) At 0.2 Hz, which is twice the heat source frequency, the frequency-domain response curves have a small peak.
(v) The point with the largest temperature change amplitude among eight temperature measurement points is the "TM housing",[a] whose temperature change amplitude only reaches 0.1249 K when the temperature amplitude of the heat source is 20 K. It shows that the system might have a good temperature control design, and the actual temperature control reaches 0.1 K@15 K $\sim$ 25 K.

These temperature responses of the temperature measurement points could be explained by a theoretical analysis. The heat transfer model could be simplified to a model of a heat source–optical platform–optical component as shown in Fig. 5 for the theoretical analysis.

In this model, it is assumed that the temperature of the heat source is $T_{\text{source}} = T_0 + T_1 \cos(\omega t)$, the optical platform temperature is $T_{\text{platform}} = T_0 + T_2(t)$ and the optical component temperature is $T_{\text{component}} = T_0 + T_3(t)$. The heat transfer power of the thermal radiation and the thermal conduction could be expressed as

$$P_{\text{radiation}} = \sigma \varepsilon A({T_{\text{source}}}^4 - {T_{\text{platform}}}^4), \tag{4}$$

$$P_{\text{conduction}} = k(T_{\text{platform}-} - T_{\text{component}}) = k(T_2 - T_3), \tag{5}$$

[a]An element, which is located at the outermost layer of the TM housing.

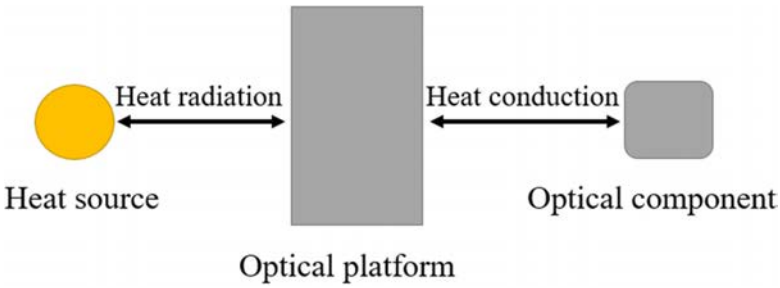

Fig. 5. The simplified heat transfer model of the Taiji-1 laser interferometer system.

where A and ε are the radiation surface area and the surface emissivity of the external heat source, respectively, and k is the heat transfer coefficient between the optical platform and the optical component. To solve the equations, a rational and simplified method is to expand Eq. (4) and take only the first- and second-order terms of T_1 and the first-order term of T_2.

According to the first law of thermodynamics, we have

$$\begin{cases} P_{\text{radiation}} - P_{\text{conduction}} = C_{\text{platform}} m_{\text{platform}} \dfrac{dT_2}{dt}, \\ P_{\text{conduction}} = C_{\text{component}} m_{\text{component}} \dfrac{dT_3}{dt}. \end{cases} \tag{6}$$

Solving Eqs. (4)–(6), we get

$$\begin{cases} T_2 = A_1 e^{-k_1 t} + B_1 + C_1 \cos(\omega t + \varphi_1) + D_1 \cos(2\omega t + \varphi_2), \\ T_3 = A_{21} e^{-k_1 t} + A_{22} e^{-k_2 t} + B_2 + C_2 \cos(\omega t + \varphi_1') + D_2 \cos(2\omega t + \varphi_2'), \end{cases} \tag{7}$$

where k_1, k_2 and $\varphi_1, \varphi_2, \varphi_1', \varphi_2'$ are only related with the system parameters and not related with T_1, while other parameters have relationships with T_1 as follows:

$$\begin{cases} A_1, A_{21}, A_{22} \propto aT_1^2 + bT_1, \\ B_1, B_2 \propto T_1^2, \\ C_1, C_2 \propto T_1, \\ D_1, D_2 \propto {T_1}^2. \end{cases} \tag{8}$$

Obviously, according to Eq. (7), the temperature frequency-domain response curves have peaks at 0.1 and 0.2 Hz, so that (ii) and (iv) could be explained by the solutions of T_2 and T_3 which contain the terms of ω and 2ω. The time-domain drift is caused by the exponential term in the solution, which could be estimated according to the system parameters. Besides, the large responses in the initial stage of the frequency-domain in (iii) are caused by the abrupt change in time-domain, while the exponential term also makes a little contribution to them.

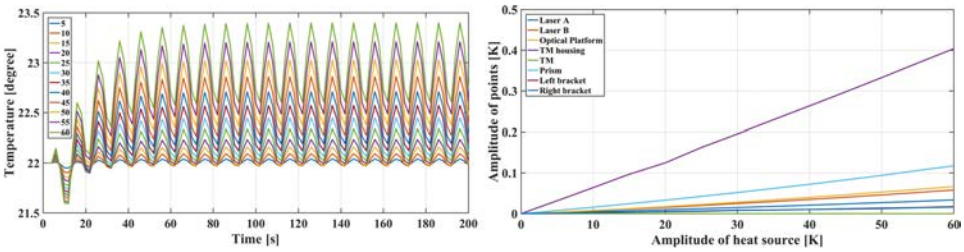

Fig. 6. *Left*: The temperature change curves of the "TM housing" temperature measurement point with time under the different external heat source temperature amplitudes. *Right*: The temperature response amplitudes of the eight temperature measurement points at 0.1 Hz with the change of the temperature amplitude of the heat source.

According to the numerical simulation results shown in the left plot of Fig. 6, it is easy to find that under the different heat source temperature amplitudes, the response phases are the same, in other words, φ_1, φ_2, $\varphi_1{}'$, $\varphi_2{}'$ are not related with T_1. Meanwhile, there is an obvious linear relationship between the temperature response amplitude at 0.1 Hz of the temperature measurement point and the heat source amplitude in the right plot, which is consistent with $C_1, C_2 \propto T_1$ in the theoretical analysis.

4.2. *The displacement response of the laser interferometer system*

On the optical platform, three nodes located on the mirror surface have been selected. The displacements in the X, Y, Z directions of the node-2 are shown in Fig. 7. The time-domain and frequency-domain responses of a single node displacement in the three directions are found similar to the temperature data. Consistent with the heat source, there are also stages of drift, oscillation and stability, and the amount of the displacement is on the order of 10 nm.

The basic law of node displacement could be explained by a theoretical analysis. For any node in the laser interferometer, the displacement in any direction could be expressed by the thermal expansion formula:

$$ds = s\alpha dT, \tag{9}$$

where α is the thermal expansion coefficient of the material, dT represents the temperature fluctuation and s is the original length of the object. Then, the node displacement in the three directions of X, Y, Z is as follows:

$$\Delta x_i \propto T_3, \quad i = 1, 2 \text{ and } 3, \tag{10}$$

so

$$\Delta x_i = A_{i1}e^{-k_1 t} + A_{i2}e^{-k_2 t} + B_i + C_i \cos(\omega t + \varphi_{1i}) + D_i \cos(2\omega t + \varphi_{2i}). \tag{11}$$

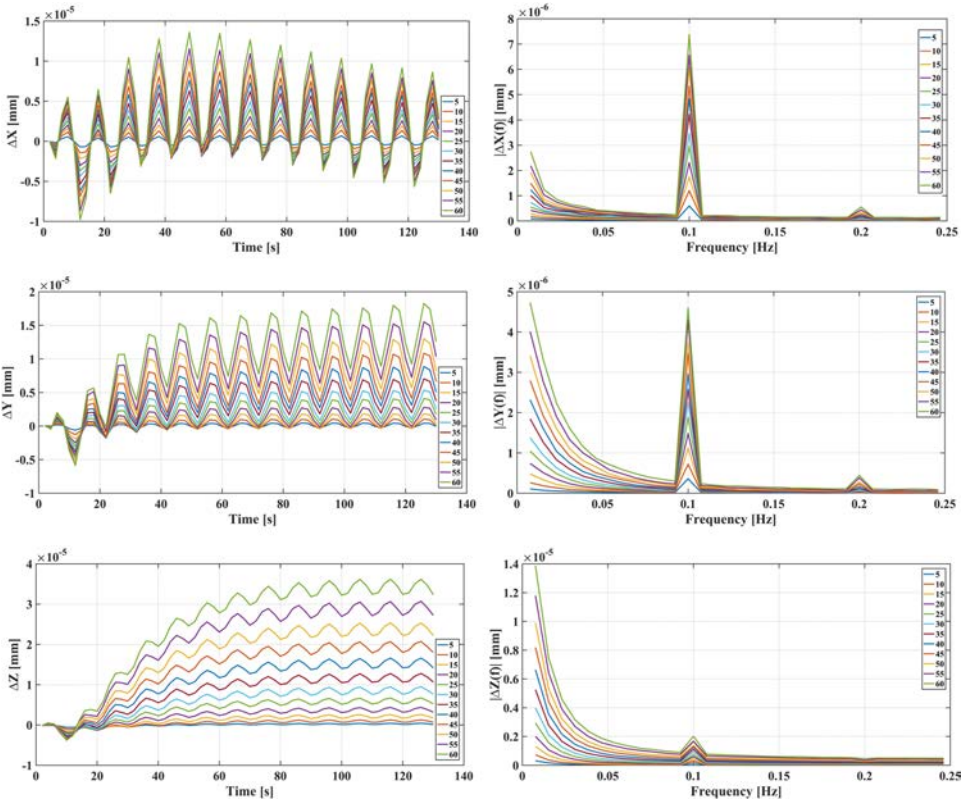

Fig. 7. *Left*: The displacement change curves of the node-2 in the X, Y, Z directions with time, under different temperature amplitudes of the heat source. *Right*: The amplitude spectrum curves after the fast Fourier transform of the displacement data (since the response amplitude is too big at 0 Hz, it is not shown in the plot).

In addition, we find from Fig. 7 that the same node has different displacements in different directions, which could also be explained. The motion of the node could be divided into two parts: the vibration of the optical platform and the vibration of the optical component where the node is located. It is obvious that the position of the optical component would affect the vibration of the optical platform, while the node position and optical component size would influence the vibration of the optical component. As a result, the node displacements in different directions are not the same, while the phenomena are also different for different nodes. According to the spatial position of the node and the size of the optical component where the node-2 is located, as shown in Fig. 8 and the above inference, the small vibration of the node-2 in the z direction could be qualitatively interpreted for the opposite direction vibrations, which makes the total vibration amplitude small.

The result shown in Fig. 9 is consistent with the theoretical analysis that $C_i \propto T_1$. Some curves in the figure do not display a perfect linear form due to the

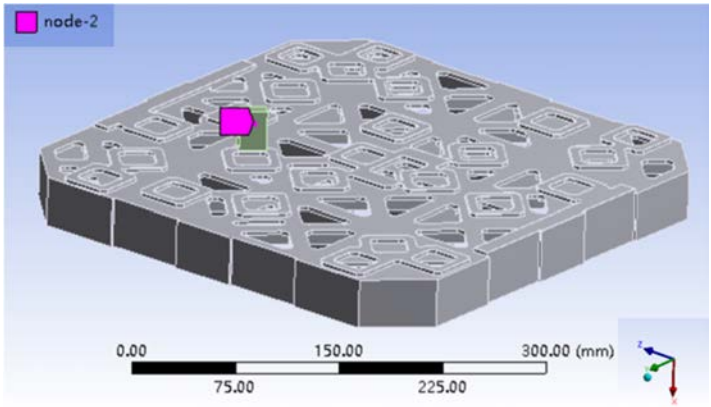

Fig. 8. The relative position of the node-2 on the optical platform of the laser interferometer, and the size of the optical component where the node-2 located is: length × width × height = 20 mm × 10 mm × 30 mm.

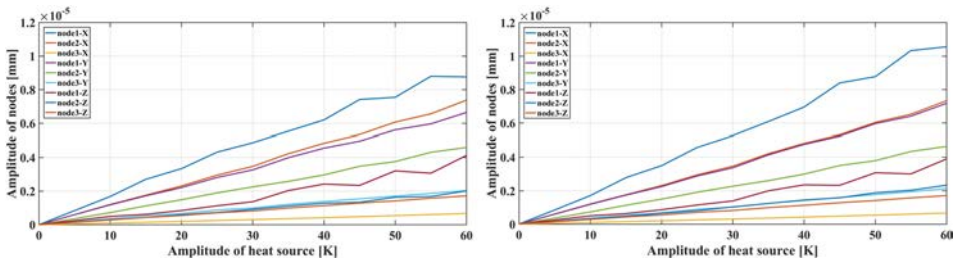

Fig. 9. *Left*: The original curves of the displacement response amplitude of the three nodes at 0.1 Hz with the change of the temperature amplitude of the heat source. *Right*: After the preliminary correction of the exponential term on the curves in the left plot.

exponential term and calculation error, while the linear relationship becomes more obvious after the preliminary elimination of the exponential term.

4.3. *The analysis of the optical path difference fluctuations*

With the optical path design and thermal–structure numerical simulation results of the laser interferometer, we obtained the fluctuations of the length difference between the two arms of each laser interferometer under different external heat source amplitudes.

According to Fig. 10, under the same heat source temperature amplitude, the time-domain and frequency-domain responses of the interference arm length difference are also consistent with the external heat source, temperature fluctuations of the temperature measurement points and the nodes displacement. When the heat source temperature amplitude is 20 K, the maximum fluctuation of the arm length difference is 36.302 nm, while the minimum is 10.367 nm. Meanwhile, the arm length difference curves also have a stage from oscillation to stability.

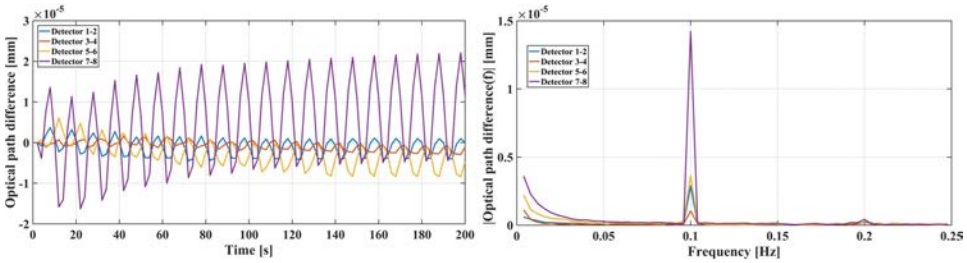

Fig. 10. The heat source temperature amplitude is 20 K. *Left*: The change curves of the interference arm length difference of each laser interferometer with time. *Right*: The amplitude spectrum curves after the fast Fourier transform of the interference arm length difference data (since the response amplitude is too big at 0 Hz, it is not shown in the plot).

Similarly, these phenomena could also be explained by a theoretical analysis. In the theoretical model, the interference arm length difference of any laser interferometer could be expressed as

$$g(t) = \sum_{i=1}^{n} k_i \Delta x_i + \sum_{i=1}^{n}\sum_{j=1}^{n} k_{i,j}\Delta x_i \Delta x_j + \sum_{i=1}^{n}\sum_{j=1}^{n}\sum_{m=1}^{n} k_{i,j,m}\Delta x_i \Delta x_j \Delta x_m + \cdots, \tag{12}$$

where $k_i, k_{i,j}, k_{i,j,m}$ are parameters only related to the properties of the optical model itself. For the first-order term of $g(t)$, the item of ω

$$g_{1\omega(t)} = \sum_{i=1}^{n} k_i C_i \cos(\omega t + \varphi_{1i}), \tag{13}$$

the amplitude of the item:

$$A_{1\omega} = \sqrt{\sum_{i=1}^{n}[k_i C_i \cos(\omega t + \varphi_{1i})]^2 + \sum_{i=1}^{n}[k_i C_i \sin(\omega t + \varphi_{1i})]^2} \propto T_1. \tag{14}$$

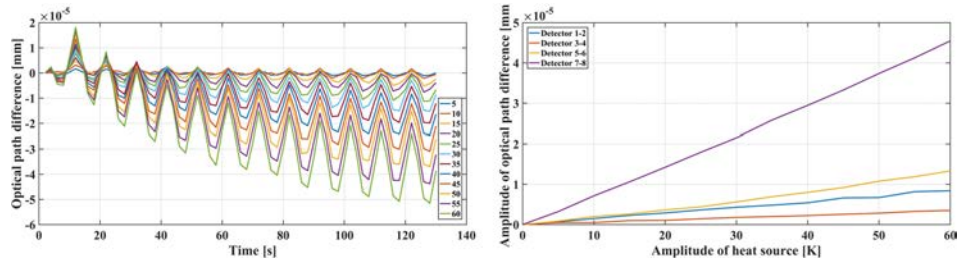

Fig. 11. *Left*: The curves of the interference arm length difference of the test interferometer with the heat source temperature amplitude. *Right*: The curves of the response amplitude of the interferometer arm length difference at 0.1 Hz with the heat source temperature amplitude for each interferometer.

Table 1. The time required for the laser interferometer optical path difference fluctuation curve to reach stable under the different heat source temperature amplitudes.

Temperature amplitude of the external heat source [K]	Time required to reach stability [s]
5	198
10	188
15	158
20	138
25	128
30	118

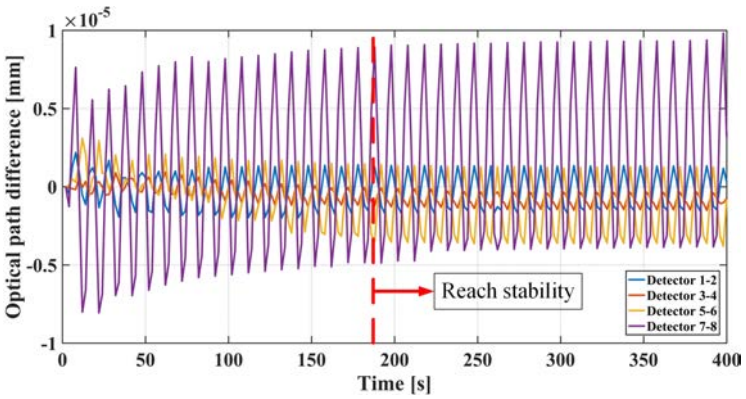

Fig. 12. (Color online) When the heat source temperature amplitude is 10 K, the time-domain response curves of the interference arm length difference for each interferometer (simulation time: 400 s), and the red dotted line presents the estimated time to reach stable.

The results shown in Fig. 11 verify that $\varphi_{1i}, \varphi_{2i}$ are not related with T_1 and $A_{1\omega} \propto T_1$ in the theoretical analysis results. The arm length difference fluctuation with the temperature amplitude of the external heat source obtained through preliminary numerical simulation exhibits an obvious linear relationship.

In addition, through a simple analysis of the time-domain curves of the arm length difference, the rough time required to reach stability for the laser interferometer system has been obtained in Table 1. Figure 12 shows the estimation of the time required for the arm length difference curves to reach stability when the temperature amplitude of the heat source is 10 K.

From Table 1, the time required to reach stability decreases with the increase of the temperature amplitude of the heat source. Moreover, the arm length difference fluctuation curves would reach stable within 130 s when the heat source temperature amplitude reaches 30 K.

4.4. *Results extension*

With the above preliminary numerical simulation results, we estimated the temperature amplitudes of the eight temperature measurement points, the displacement

Table 2. The estimated temperature amplitudes of the eight temperature measurement points, the displacement amplitudes of the three nodes and the interference arm length difference of each laser interferometer, when the temperature amplitude of the external heat source is 0.1 K, are shown.

Estimated temperature amplitudes of the eight temperature measurement points/[mK]							
Laser A	Laser B	Optical platform	TM housing	TM	Prism	Left bracket	Right bracket
0.05299	0.08937	0.1017	0.6618	0.00	0.1842	0.02631	0.02587

Estimated displacement amplitudes of the three nodes/[pm]								
Node-1			Node-2			Node-3		
X1	Y1	Z1	X2	Y2	Z2	X3	Y3	Z3
17.91	11.74	5.665	11.95	7.651	3.624	1.056	3.51	2.815

Estimated interference arm length difference of the four laser interferometer/[pm]			
Detector 1–2	Detector 3–4	Detector 5–6	Detector 7–8
14.17	5.776	20.82	74.27

of the three nodes and the response amplitudes of the arm length difference of each laser interferometer under the condition of actual temperature control of Taiji-1 laser interferometer system, where the external heat source temperature amplitude $\Delta T = 0.1\,\mathrm{K}$.

According to the preliminary estimations in Table 2, we find that under this condition, the temperature fluctuation amplitudes in the system would be below the order of mK, the node displacement would be within 100 pm, and the fluctuation amplitudes of the arm length difference would also be within 100 pm.

5. Conclusion

The preliminary simulation results of Taiji-1 temperature fluctuation noise are consistent with the theoretical analysis, which shows that the numerical simulation scheme we used should be reasonable and feasible. With the scheme, the temperature fluctuation noise of the space-borne laser interferometer could be estimated and analyzed preliminarily.

However, according to the simulation results obtained so far, there are many defects that needed further improvement in the scheme. The finite element model of the laser interferometer should be optimized and a more accurate thermal–structure–optical simulation method should be selected in the following research. Furthermore, the influence of the other two mechanisms of the temperature fluctuation noise needs to be considered. We will continue to study the responses of the interferometer output signal under the action of the external heat source, and further look for the relationships between the interferometer output signal and the system temperature fluctuation.

Acknowledgments

This work was financially supported by the Strategic Priority Research Program of the Chinese Academy of Sciences (Grant Nos. XDA1502070902, XDA1502070304 and XDA1501800003).

References

1. K. Danzmann *et al.*, *Class. Quantum Grav.* **13**, A247 (1996).
2. K. Danzmann *et al.*, Albert Einstein Institute Hannover, Leibniz University Hannover, Max Planck Institute Gravitational Physics, Hannover, Germany, Tech. Rep. (2017).
3. K. Danzmann *et al.*, Max-Planck-Institut für Quantenoptik, Report No. MPQ 208 (1998), p. 57.
4. O. Jennrich *et al.*, ESA/SRE 19 (2011).
5. W.-R. Hu and Y.-L. Wu, The Taiji program in space for gravitational wave physics and the nature of gravity (2017).
6. Z. Luo, Z. Guo, G. Jin, Y. Wu and W. Hu, *Results Phys.* **16**, 102918 (2020).
7. Z. Luo, H. Liu and G. Jin, *Opt. Laser Technol.* **105**, 146 (2018).
8. Z. Luo *et al.*, *Adv. Mech.* **43**, 415 (2013).
9. M. Nofrarias, A. G. Marín, G. Heinzel, M. Hewitson, A. Lobo, J. Sanjuán, J. Ramos-Castro and K. Danzmann, *J. Phys. Conf. Ser.* **154**, 012004 (2009).
10. H. Peabody and S. M. Merkowitz, *AIP Conf. Proc.* **873**, 204 (2006).
11. F. Gibert *et al.*, *Class. Quantum Grav.* **32**, 045014 (2015).
12. M. Nofrarias Serra, *Thermal Diagnostics in the LISA Technology Package Experiment* (Universitat de Barcelona, 2007).
13. A. Lobo, M. Nofrarias, J. Ramos-Castro and J. Sanjuan, *Class. Quantum Grav.* **23**, 5177 (2006).
14. A. Lobo, M. Nofrarias, J. Ramos-Castro and J. Sanjuan, arXiv:gr-qc/0601096.
15. H. Peabody and S. Merkowitz, *Class. Quantum Grav.* **22**, S403 (2005).
16. S. Vitale *et al.*, University of Trento, document code Unitn-Int 10 (2002).
17. F. Gibert, M. Nofrarias, M. Diaz-Aguiló, A. Lobo, N. Karnesis, I. Mateos, J. Sanjuán, I. Lloro, L. Gesa and V. Martín, *J. Phys. Conf. Ser.* **363**, 012044 (2012).

18. F. Gibert *et al.*, In-flight thermal experiments for LISA pathfinder: Simulating temperature noise at the inertial sensors, in *10th Int. LISA Symp.* (*LISAX*) (2015).
19. F. Gibert, M. Nofrarias, N. Karnesis, M. Díaz-Aguiló, I. Mateos, A. Lobo, L. Gesa, V. Martín and I. Lloro, arXiv:1312.3191.
20. P. Hello and J.-Y. Vinet, *Phys. Lett. A* **178**, 351 (1993).
21. J. Holman, *Heat Transfer*, 10th edn. (2010).